The first case of actinide polyrotaxane incorporating cucurbituril: A unique 'dragon-like' twist induced by a specific coordination pattern of uranium

Lei Mei,[a] Qun-yan Wu,[a] Cai-ming Liu,[b] Yu-liang Zhao,[a] Zhi-fang Chai*[ac], Wei-qun Shi*[a]

Supporting Information

Table of contents

S1. General Methods

Caution! Suitable measures for precautions and protection should be taken, and all operations should follow the criteria while handling such substances although natural uranium was used in the experiment. Cucurbit[6]uril (CB[6]) was synthesized according to reference[1]. All other reagents were purchased from commercial sources and used as received.

^{1}H-NMR spectra were recorded on a Bruker AVANCE III (500 MHz, Bruker, Switzerland) with deuterium oxide as a solvent. ESI-MS spectra were obtained with a Bruker AmaZon SL ion trap mass spectrometer (Bruker, USA). The Fourier transform infrared (FT-IR) spectra were recorded from KBr pellets in the range of 4000-400 cm^{-1} on at Bruker Tensor 27 spectrometer. Raman spectra were recorded from 4500 to 100 cm^{-1} on a Horiba LabRAM HR Evolution Microscopic Confocal Raman spectrometer with a 473 nm argon ion laser. Solid-state fluorescence spectra were measured on a Hitachi F-4600 fluorescence spectrophotometer. The morphology of crystal was observed with SEM (S-4800, HITACHI) at an accelerating voltage of 1.0 kV. Powder XRD measurements were recorded on a Bruker D8 Advance diffractometer with Cu Kα radiation (λ=1.5406 Å) in the range 5-80°(step size: 0.02º). Thermogravimetric analysis (TGA) was performed on a TA Q500 analyzer over the temperature range of 20-900 °C in air atmosphere with a heating rate of 3.00 °C/min.

Preparation of C4CN3 and C4CN3-CB6

The compounds of **C4CN3 and C4CN3-CB6** were synthesized according to the procedures reported previously[2].

C4CN3: 3-Cyanobenzaldehyde (1.00 g, 7.63 mmol) was added to a solution of 1, 4-diaminobutane (0.32g, 3.63 mmol) in methanol (50 mL) and the mixture was heated at reflux for 12 h. $NaBH_4$ (0.50 g, 13.2 mmol) was added carefully in batches and the mixture was refluxed for another 12 h. The solvent was removed in vacuo and the white residue was dissolved in a small amount of distilled water. After the aqueous solution was basified with 0.5 M NaOH, the product was extracted with dichloromethane twice. The extract was dried over magnesium sulfate and evaporated in vacuo. The while solid was dissolved in ethanol followed by addition of excess amount of HNO_3. The precipitate the product was then filtered, washed with ethanol and dried in vacuo to obtain **C4CN3** (1.55g, 96%). IR (KBr): υ(C-H) 3051, 2853; υ(C≡N) 2234; υ(CH_2) 1476;

υ(C-N) 1382; υ(Ph-H) 809, 691 cm^{-1}. ^1H NMR (500MHz, D_2O, δ ppm): 8.00 (m, 4H), 7.92 (m, 2H), 7.80 (m, 2H), 4.44 (s, 4H), 3.26 (m, 4H), 1.92 (m, 4H). MS (ESI): mass calculated for $C_{20}H_{22}N_4^{2+}$ (M^{2+}), 320.20; m/z found, 319.04 ($[M-H]^+$)

1 (C4CN3-CB6): To a solution of **C4CN3** (0.500 g, 1.13 mmol) in water (150 mL) was added CB[6] (1.30 g, 1.31 mmol). The mixture was refluxed for 4 h. Undissolved CB[6] was filtered off and the volume of the filtrate was reduced to about 50 mL during which considerable amount of colorless crystals arise. Ethanol (200 mL) was added to the solution to precipitate more product and the light yellow crystals were filtered, washed with EtOH and dried in vacuo (0.84 g, 56%). IR (KBr): υ(C-H) 2922, 2853; υ(C≡N) 2232; υ(C=o) 1733; υ(CH_2) 1474; υ(C-N) 1384, 1321, 1233, 1188; υ(Ph-H) 802 cm^{-1}. ^1H NMR (500MHz, D_2O, δ ppm): 8.24 (m, 2H); 8.13 (m, 2H), 7.92 (m, 2H), 7.73 (m, 2H), 5.75 (d, 12H), 5.68 (s, 12H), 4.48 (s, 4H), 4.41 (d, 4H), 2.54 (s, 4H), 0.66 (s, 4H). MS (ESI): mass calculated for $C_{56}H_{60}N_{28}O_{12}$ (M^{2+}) , 1316.50; m/z found, 658.21 (M^{2+}).

Pseudorotaxane precusor (see the Supporting Information) was dissolved in water and the aqueous solution was allowed to evaporate at room temperature to obtain the crystal of **1** suitable for single crystal diffraction after 2 weeks.

2 (UO2-C4CA3-CB6): $UO_2(NO_3)_2 \cdot 6H_2O$ (140 μL, 0.07 mmol) were added to a suspension of **1** (0.10 g, 0.07 mmol) in water (2 mL) in a stainless-steel bomb. After treating with HNO_3 or triethylamine, the mixture was sealed, kept at 180°C for 72 h and cooled to room temperature. Light yellow crystals **2** were washed with water and ethanol and dried in air (56 mg, 48%).

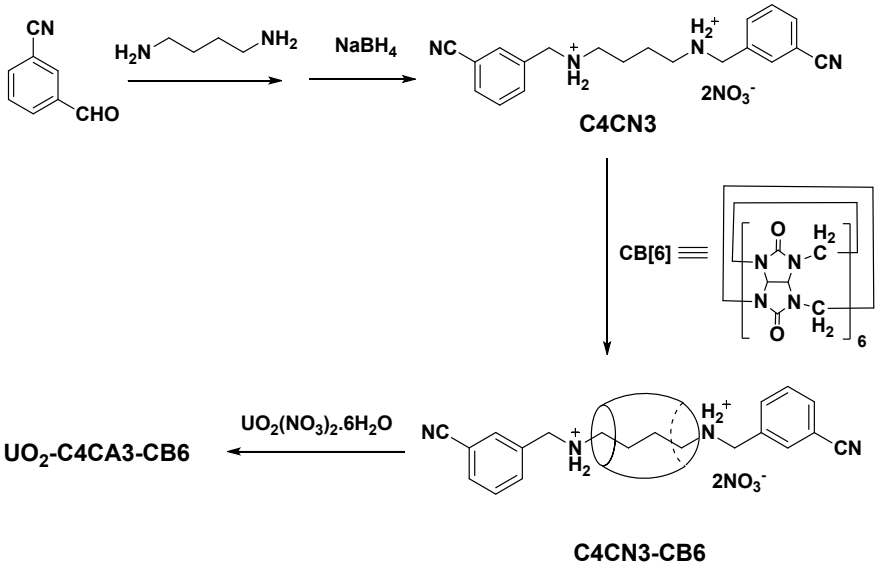

Scheme S1. Synthesis of **C4CN3**, **C4CN3-CB6** and **UO_2-C4CA3-CB6**.The barrel-like cartoon in

the molecular structure represents a simplified depiction of CB[6].

^{1}H NMR spectra for C4CN3 and C4CN3-CB6

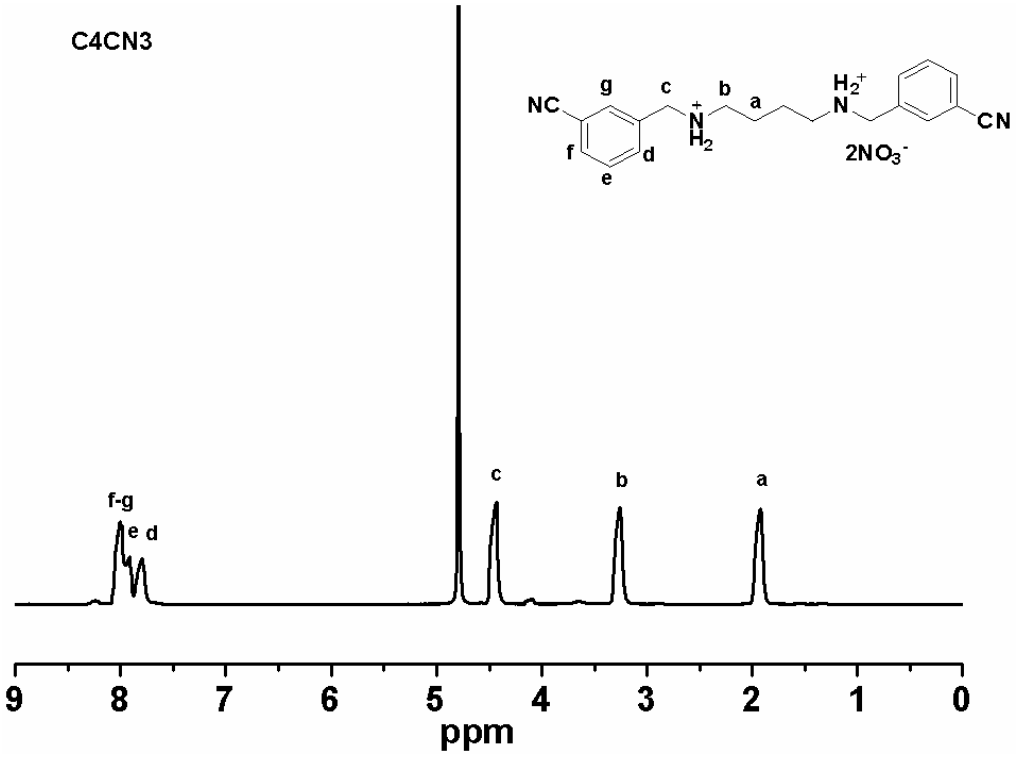

Fig. S1. ^{1}H NMR spectrum of **C4CN3** (500 MHz in D_2O)

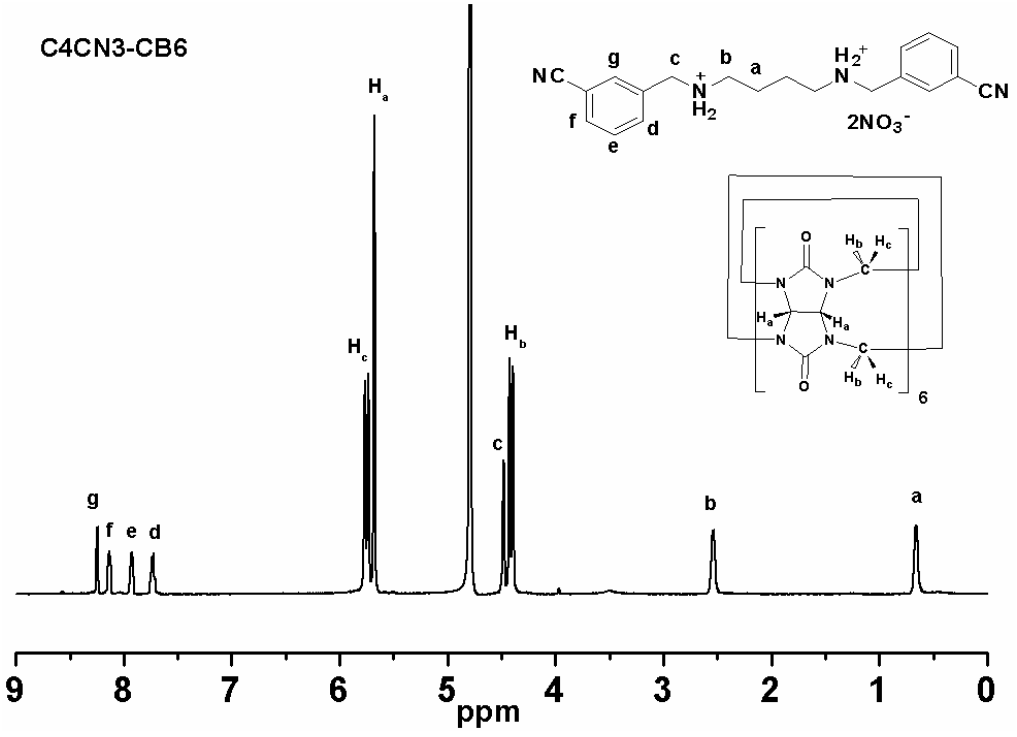

Fig. S2. ^{1}H NMR spectrum of **C4CN3-CB6** (500 MHz in D_2O)

X-ray Single Structural Determination

X-ray diffraction data of pseudorotaxane **1** (C4CN3-CB6) were collected on a Bruker APEXII X-ray CCD diffractometer with a Mo Kα X-ray source (λ = 0.71073 Å) at room temperature. Standard APEXII software was used for determination of the unit cells and data collection control. The crystal structures were solved by means of direct methods and refined with full-matrix least squares on SHELXL-97. Crystal data for **1**: $C_{56}H_{74}N_{30}O_{25}$, $(C_{20}H_{24}N_4@C_{36}H_{36}N_{24}O_{12})(NO_3)_2•7(H_2O)$, Mr = 1567.45, Monoclinic, C2/c, a =26.608(4) Å, b = 20.323(3) Å, c = 13.2407(18) Å, β= 114.223(3)°, V = 6529.6(15)Å^3, Z = 4, $\rho_{calcd.}$= 1.594 gcm^{-3}. The crystal structures were solved by means of direct methods and refined with full-matrix least squares on SHELXL-97 and converged to R_1 = 0.0744 and wR_2 = 0.2090, and GOF = 1.049 (Rint = 0.0514) for 18581 reflections [I > 2σ(I)].

Data collection of the uranyl compound **2 (**UO_2-C4CA3-CB6) was performed with synchrotron radiation facility at BSRF (beamline 3W1A of Beijing Synchrotron Radiation Facility, λ = 0.71073 Å) using a MAR CCD detector. The crystal was mounted in nylon loops and cooled in a cold nitrogen-gas stream at 100 K. Data were indexed, integrated and scaled using DENZO and SCALEPACK from the HKL program suite (Otwinowski & Minor, 1997). The crystal structures were solved by means of direct methods and refined with full-matrix least squares on SHELXL-97. Crystal data for **2**: $C_{56}H_{62}N_{26}O_{20}U$, $UO_2(H_2O)_2(\eta^2\text{-}C_{20}H_{22}N_2O_4@C_{36}H_{36}N_{24}O_{12})_{0.5}(\eta^1\text{-}C_{20}H_{22}N_2O_4@C_{36}H_{36}N_{24}O_{12})_{0.5}$, Mr = 1657.35, Monoclinic, $P2_1/c$, a =12.887(3) Å, b = 19.363(4) Å, c = 25.334(8) Å, β= 115.53(3)°, V = 5704(3)Å^3, Z = 4, ρ_{calcd} = 1.930 gcm^{-3}, The crystal structures were solved by means of direct methods and refined with full-matrix least squares on SHELXL-97 and converged to R_1 = 0.1178 and wR_2 = 0. 03172, and GOF = 1.111. (Rint = 0.0702) for 15963 reflections [I > 2σ(I)].

Reference

1. Day, A.; Arnold, A. P.; Blanch, R. J. and Snushall, B. J. Org. Chem., **2001**, 66, 8094 – 8100;
2. Kim, J.; Jung, In-S.; Kim, S. Y.; Lee, E.; Kang, J. K.; Sakamoto, S.; Yamaguchi, K. and Kim, K. J. Am. Chem. Soc., **2000**, 122, 540 – 541.

S2. Typical figures and data

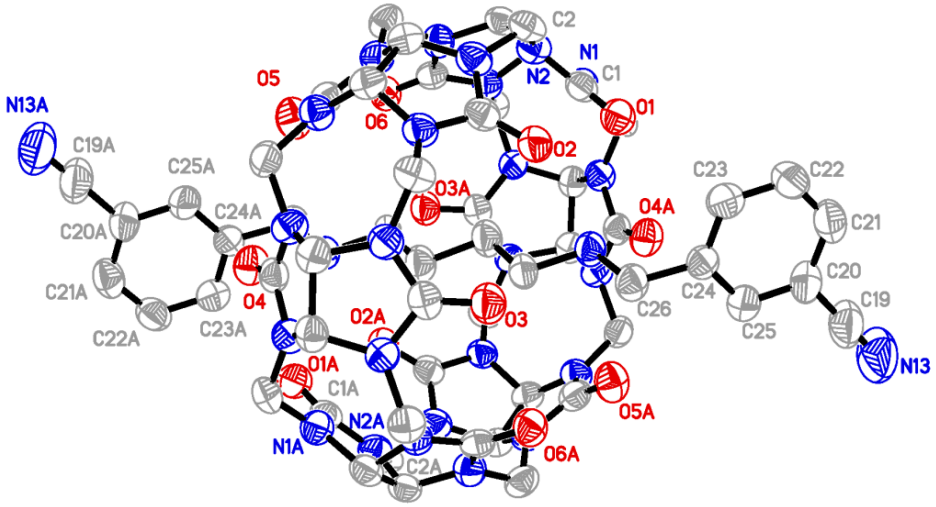

Fig. S3. ORTEP drawing of the asymmetric unit of C4N3-CB6. Thermal ellipsoids are shown at 50% probability. All hydrogen atoms are omitted for clarity.

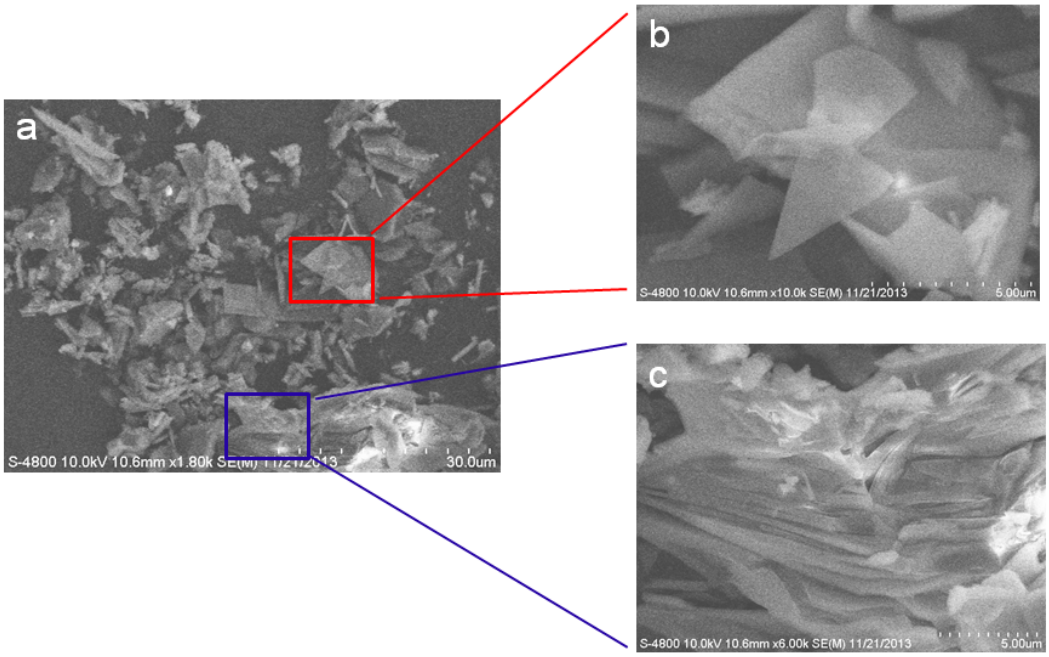

Fig. S4. SEM images of UO_2-C4A3-CB6 (a) and enlarged drawing of different regions (b: scattered schistose crystal; c: stacked schistose crystal).

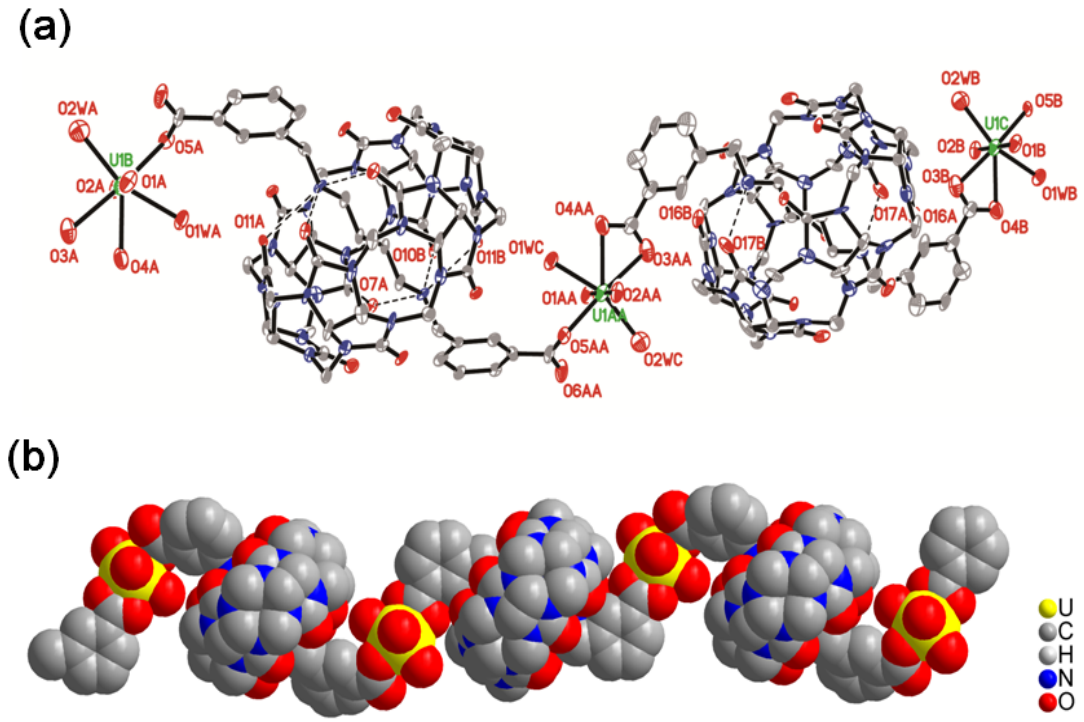

Fig. S5. ORTEP drawing (a) and space-filling representation (b) of UO_2-C4A3-CB6 with CB[6]-encapsuted structural units. Hydrogen atoms are omitted for clarity. Symmetry transformations used to generate equivalent atoms: #1 -x+2,-y,-z+1; #2 -x-1,-y,-z; #3 -x+1,-y,-z; #4 -x,-y+1,-z.

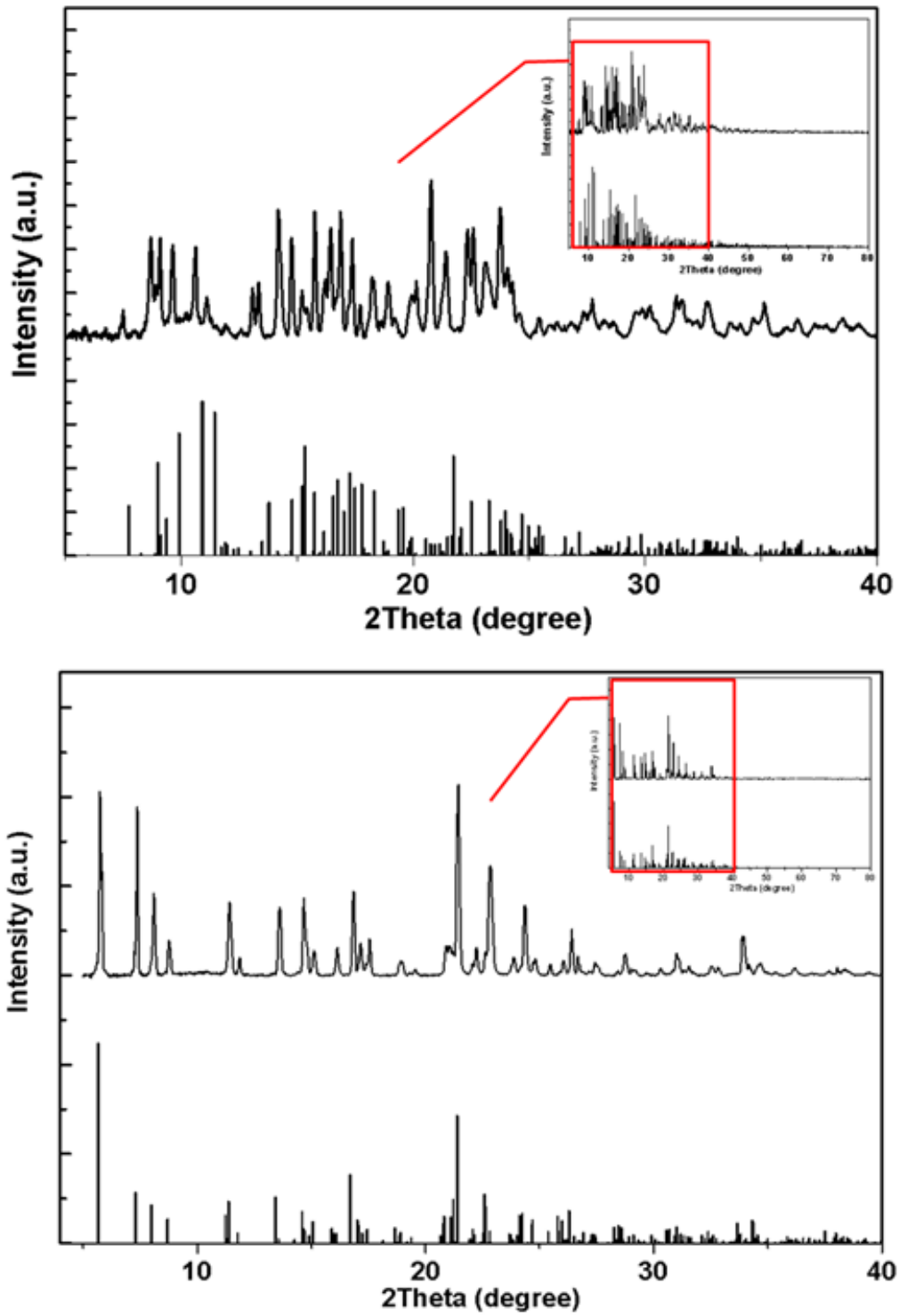

Fig. S6. Powder-XRD results for **2** (UO_2-C4A3-CB6) (top) and **1** (C4N3-CB6) (bottom). Insert: Power-XRD diagram in the range 5-80°. The upper and lower parts for each diagram are experimental spectra and simulated spectra from single crystal data.

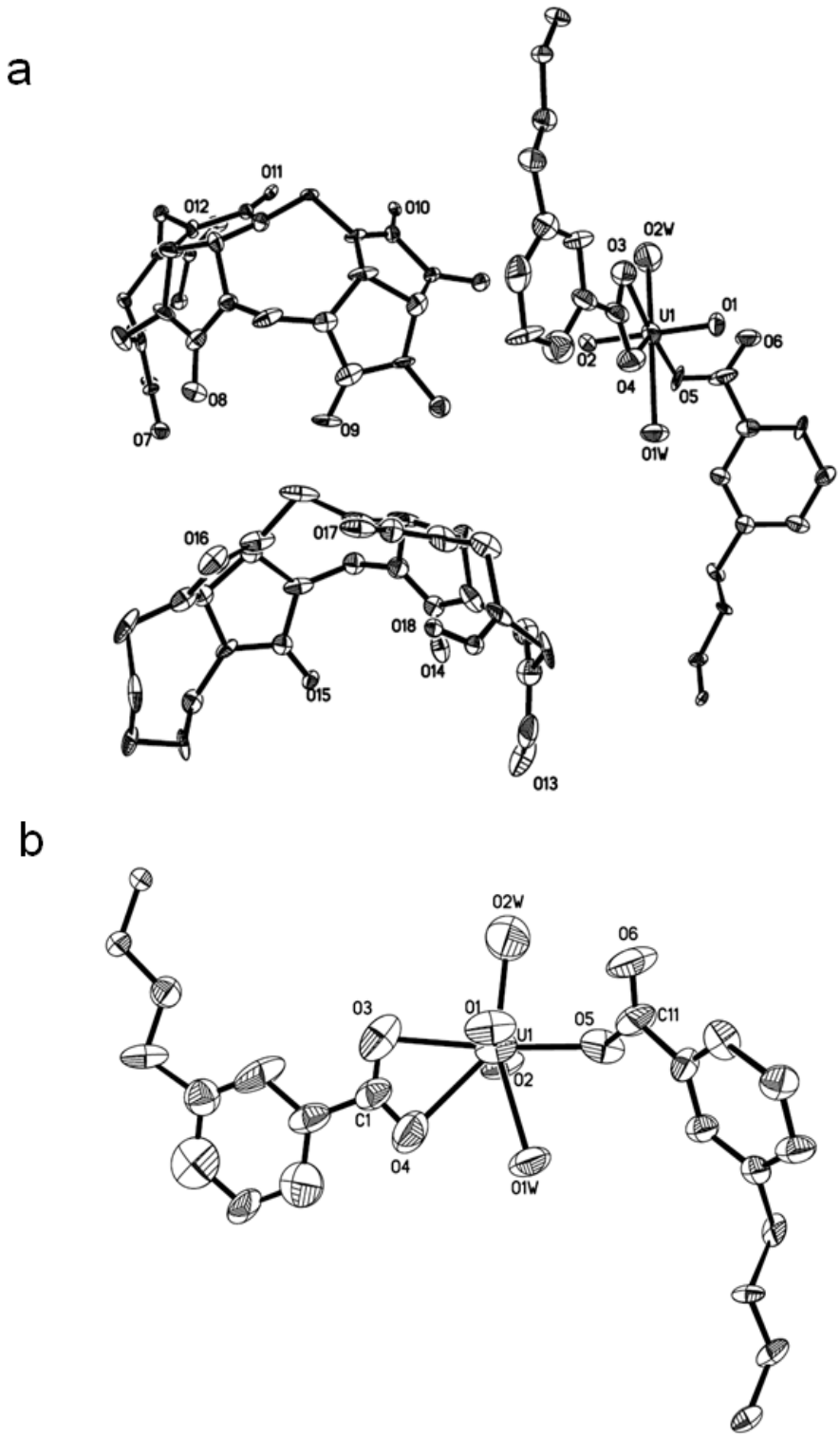

Fig. S7. ORTEP drawing of UO_2-C4A3-CB6: (a) the asymmetric unit, thermal ellipsoids are shown at 30% probability; (b) the uranyl coordination sphere. All hydrogen atoms are omitted for clarity.

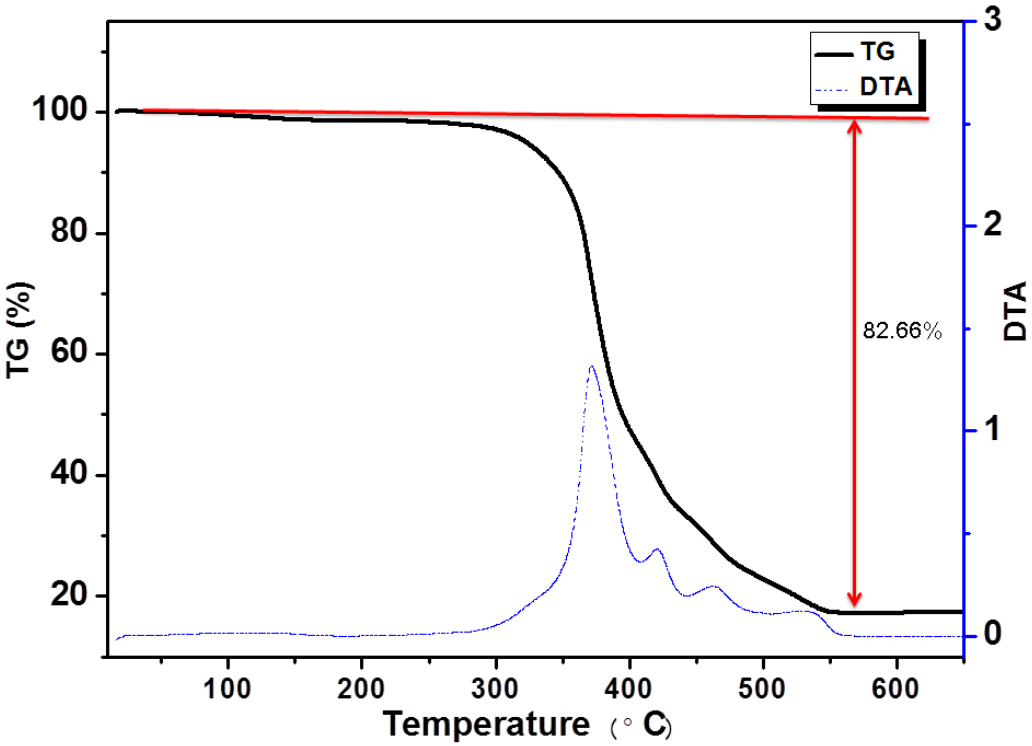

Fig. S8. Thermogravimetric results for **2** (UO_2-C4A3-CB6). The total weight loss of 82.66% after heating up to 650 °C is close to theoretical value of 83.06 %.

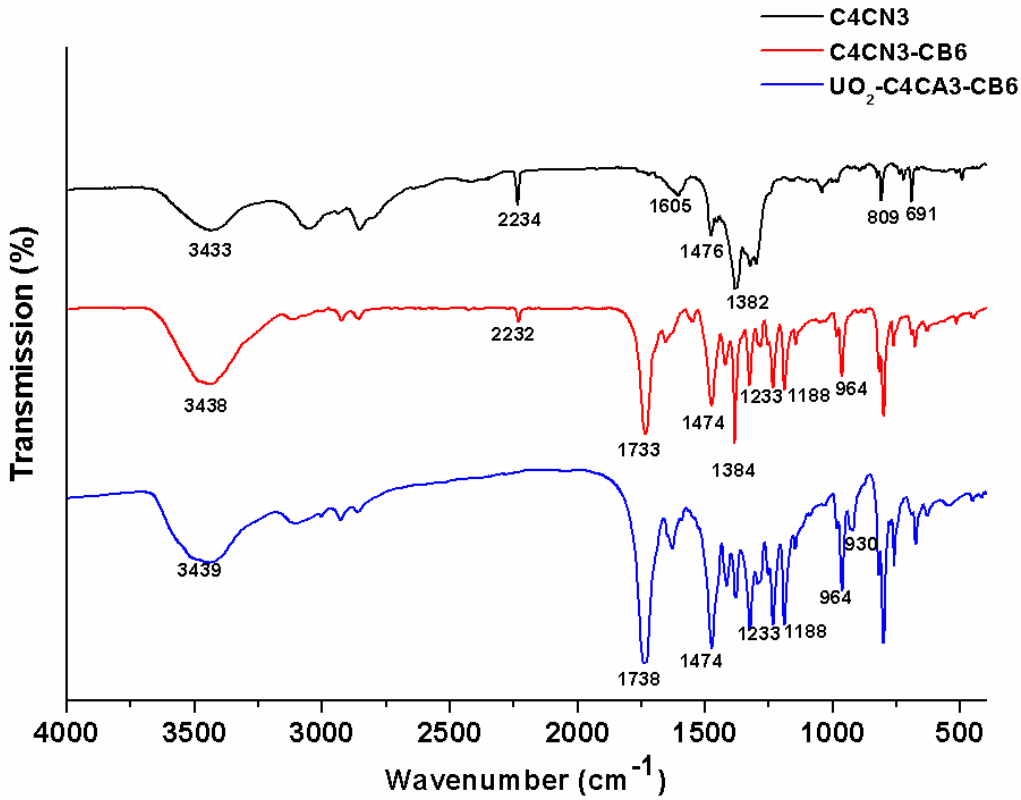

Fig. S9. The IR spectrum of C4CN3, **1** (C4CN3-CB6), **2** (UO_2-C4A3-CB6).

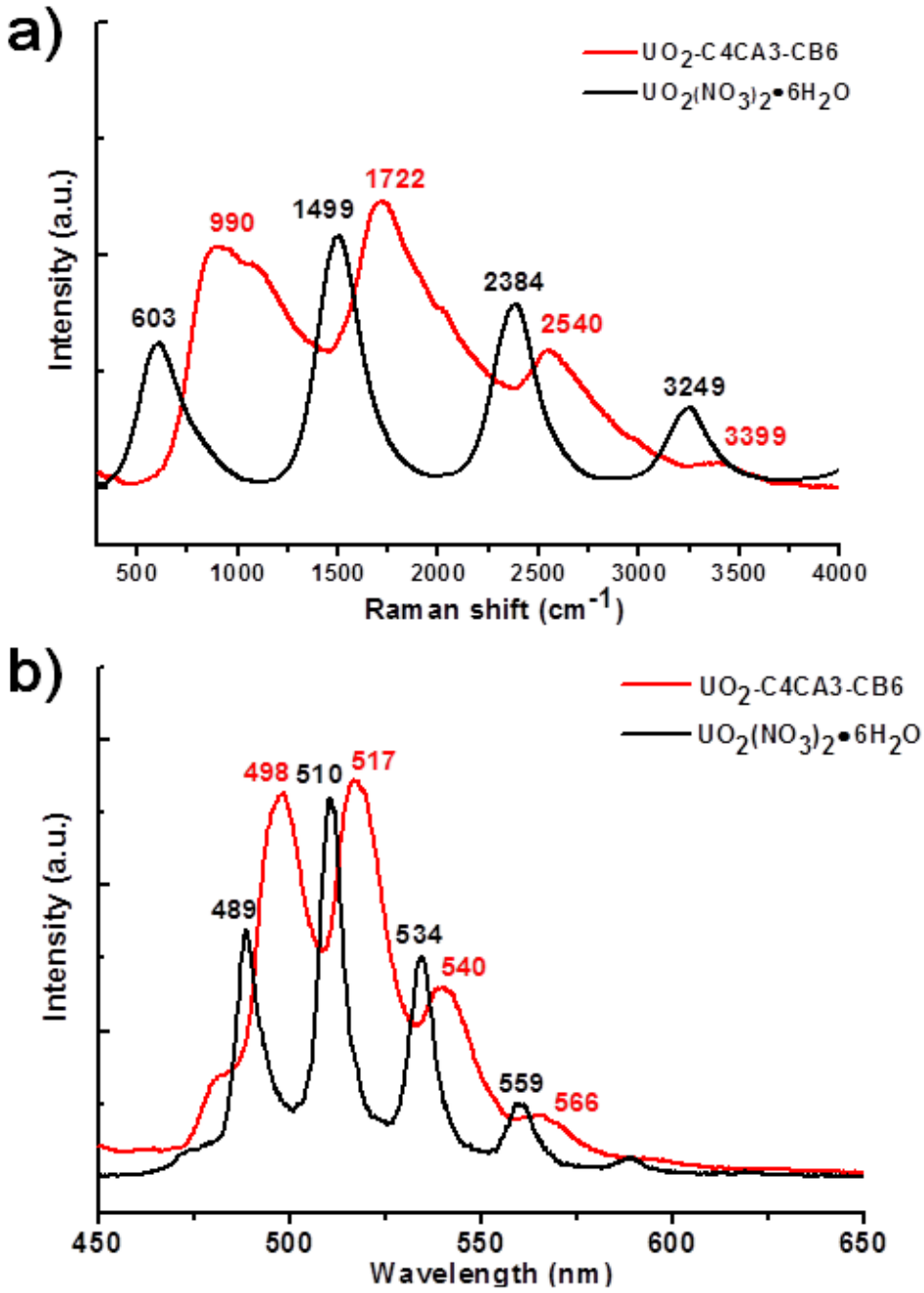

Fig. S10. Raman and fluorescence spectrum of **2** (UO_2-C4A3-CB6) and $UO_2(NO_3)_2 \cdot 6H_2O$. There is a separation of about 803 cm^{-1} (mean value) between two adjacent fingerprinted peaks for **2** (UO_2-C4A3-CB6), which can be related to the [U=O] stretching vibration, and a slight red shift can be found compared to $UO_2(NO_3)_2 \cdot 6H_2O$.

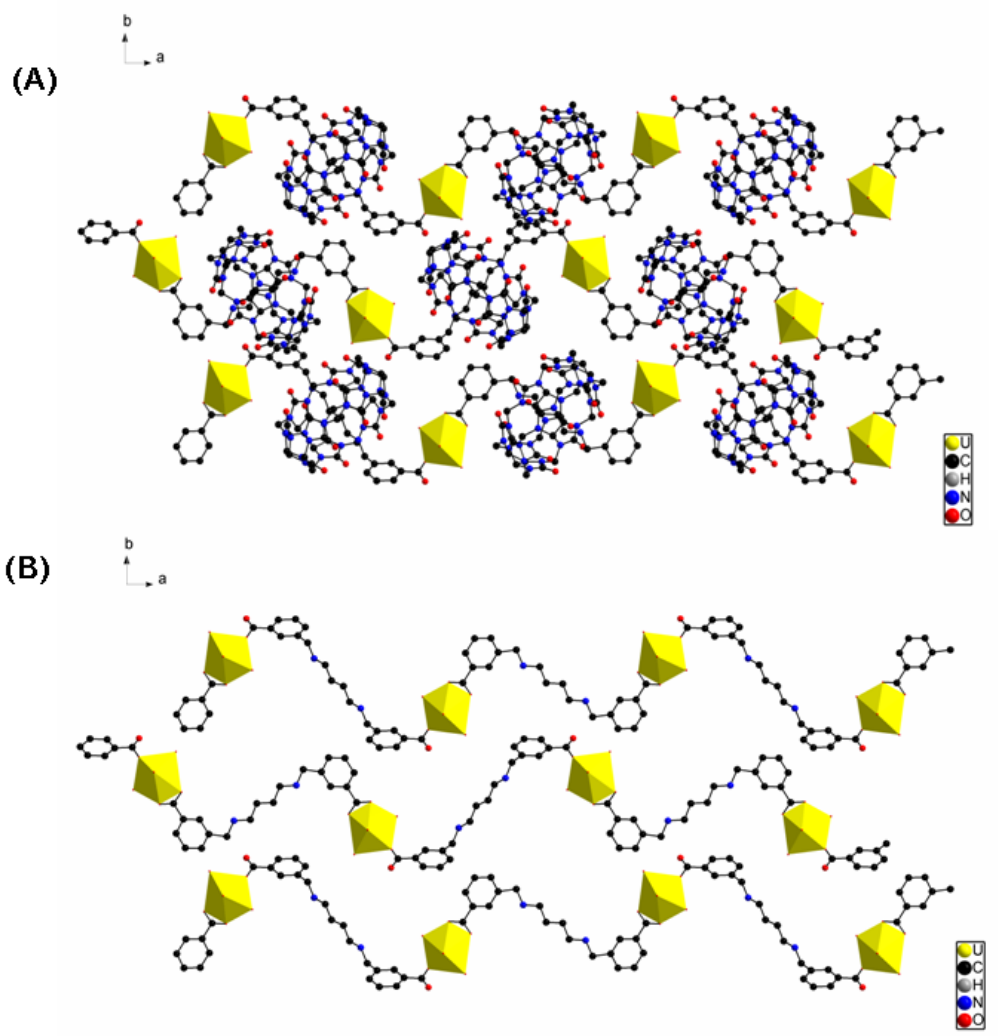

Fig. S11. View of packing diagram in **2** (UO_2-C4CA3-CB6) viewing along c axis. (A: packing polymers with CB[6]; B: packing polymers without CB[6];)Uranyl is represented as pentagonal bipyramids in yellow, while O atoms in red, N atoms in blue and C atoms in black. Hydrogen atoms are omitted for clarity.

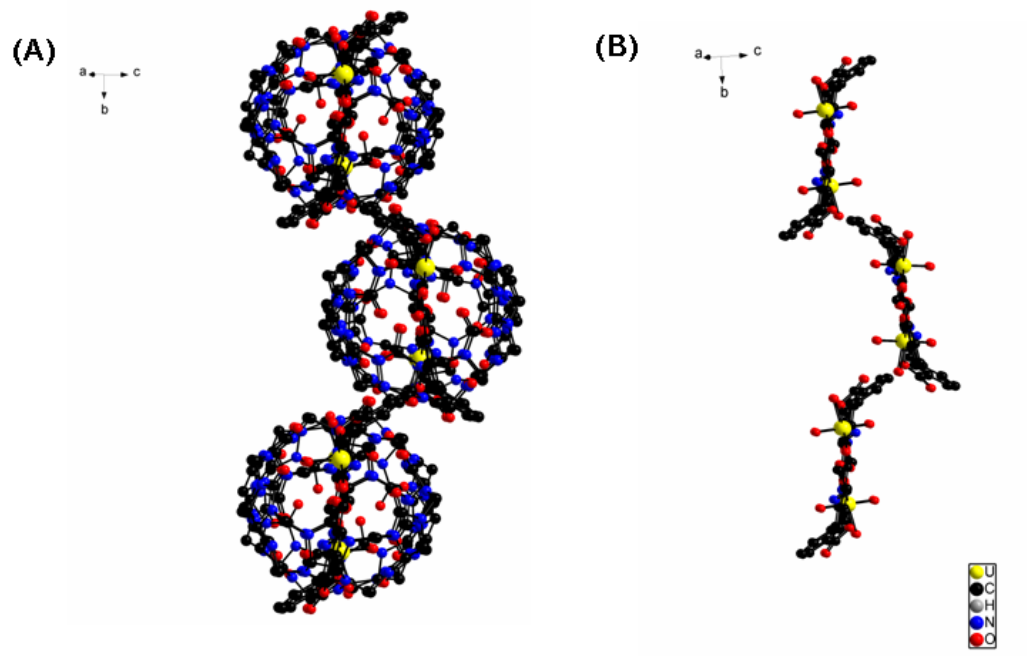

Fig. S12. View of packing diagram in **2** viewing from a diagonal direction. (A: packing polymers with CB[6]; B: packing polymers without CB[6];)Uranyl is represented as pentagonal bipyramids in yellow, while O atoms in red, N atoms in blue and C atoms in black. Hydrogen atoms are omitted for clarity.

S3. Quantum chemistry calculation

Two model fragments were selected where model A includes the uranyl, 'axle' ligand and CB[6] and model B does not contain CB[6]. Because model A is relative larger atoms, the optimization were carried out using ONIOM, which is the hybrid method that enables different theory level to be applied to the different parts of a system.[1] ONIOM computational approach was found particularly useful for transition metal complexes.[2] The higher layer of the model A is using quantum method and the lower layer is simulated by UFF.

The geometry optimizations for quantum mechanics were carried out using DFT method with the Gaussian 09 program[3] and the hybrid exchange-correlation function B3LYP was employed,[4,5] which have evolved as a practical and effective computational tool for large actinide compounds.[6-8] For geometry optimizations, the small-core quasi-relativistic pseudo-potential ECP60MWB and associated ECP60MWB-SEG valence basis sets were applied for uranium,[9-11] while the 6-31G(d) basis set was used for the other light atoms H, C, N and O. The small-core pseudopotential replaces 60 core electrons for uranium while the remaining 32 electrons were represented by the associated valence basis set. It was shown that the small-core ECPs are much more reliable for investigations of the thermochemistry of uranium fluorides than large-core ECPs.[12] Harmonic vibrational frequencies were calculated to confirm the optimized structures as the local minima on the potential energy surfaces.

References:

1. S. Dapprich, I. Komaromi, K.S. Byun, K. Morokuma, and M.J. Frisch Journal of Molecular Structure: THEOCHEM. (1999), 461-462.

2. Ananikov, Valentine P.; Musaev, Djamaladdin G.; Morokuma, Keiji Journal of Molecular Catalysis A: Chemical 324 (2010) 104–119

3. Frisch, M. J. T., G. W.; Schlegel, H. B.; Scuseria, G. E.; Robb, M. A.; Cheeseman, J. R.; Scalmani, G.; Barone, V.; Mennucci, B.; Petersson, G. A.; Nakatsuji, H.; Caricato, M.; Li, X.; Hratchian, H. P.; Izmaylov, A. F.; Bloino, J.; Zheng, G.; Sonnenberg, J. L.; Hada, M.; Ehara, M.; Toyota, K.; Fukuda, R.; Hasegawa, J.; Ishida, M.; Nakajima, T.; Honda, Y.; Kitao, O.; Nakai, H.; Vreven, T.; Montgomery, Jr., J. A.; Peralta, J. E.; Ogliaro, F.; Bearpark, M.; Heyd, J. J.; Brothers, E.; Kudin, K. N.;

Staroverov, V. N.; Kobayashi, R.; Normand, J.; Raghavachari, K.; Rendell, A.; Burant, J. C.; Iyengar, S. S.; Tomasi, J.; Cossi, M.; Rega, N.; Millam, N. J.; Klene, M.; Knox, J. E.; Cross, J. B.; Bakken, V.; Adamo, C.; Jaramillo, J.; Gomperts, R.; Stratmann, R. E.; Yazyev, O.; Austin, A. J.; Cammi, R.; Pomelli, C.; Ochterski, J. W.; Martin, R. L.; Morokuma, K.; Zakrzewski, V. G.; Voth, G. A.; Salvador, P.; Dannenberg, J. J.; Dapprich, S.; Daniels, A. D.; Farkas, Ö.; Foresman, J. B.; Ortiz, J. V.; Cioslowski, J.; Fox, D. J.; Gaussian, I., Wallingford CT, Ed. 2009.
4. Becke, A. D. *Phys. Rev. A* **1988**, *38*, 3098.
5. Lee, C. T.; Yang, W. T.; Parr, R. G. *Phys. Rev.B* **1988**, *37*, 785.
6. Lan, J.-H.; Shi, W.-Q.; Yuan, L.-Y.; Zhao, Y.-L.; Li, J.; Chai, Z.-F. *Inorg. Chem.* **2011**, *50*, 9230.
7. Wang, C.-Z.; Lan, J.-H.; Zhao, Y.-L.; Chai, Z.-F.; Wei, Y.-Z.; Shi, W.-Q. *Inorg. Chem.* **2013**, *52*, 196.
8. Wang, C.-Z.; Shi, W.-Q.; Lan, J.-H.; Zhao, Y.-L.; Wei, Y.-Z.; Chai, Z.-F. *Inorg. Chem.* **2013**, *52*, 10904.
9. Küchle, W.; Dolg, M.; Stoll, H.; Preuss, H. *J. Chem. Phys.* **1994**, *100*, 7535.
10. Cao, X.; Dolg, M.; Stoll, H. *J. Chem. Phys.* **2003**, *118*, 487.
11. Cao, X.; Dolg, M. *Journal of Molecular Structure: THEOCHEM* **2004**, *673*, 203.
12. Batista, E. R.; Martin, R. L.; Hay, P. J.; Peralta, J. E.; Scuseria, G. E. *J. Chem. Phys.* **2004**, *121*, 2144.

Table. S1. Bond lengths and angles of experimental crystallographic data and data from quantum chemical computation

	Experimental	model B	model A
U(1)-O(2)	1.650(13)	1.77630	1.76649
U(1)-O(1)	1.650(13)	1.77362	1.77496
U(1)-O(5)	2.186(15)	2.27774	2.38510
U(1)-O(2W)	2.326(18)	2.52231	2.44381
U(1)-O(1W)	2.398(13)	2.51371	2.56646
U(1)-O(3)	2.418(16)	2.43092	2.37016
U(1)-O(4)	2.445(17)	2.42601	2.43402
O(5)-U(1)-O(2W)	85.0(6)	69.37885	50.75745
O(5)-U(1)-O(1W)	72.8(5)	50.39150	66.02096
O(2W)-U(1)-O(3)	90.3(7)	69.61276	84.54472
O(1W)-U(1)-O(4)	62.7(5)	81.67230	78.11645
O(3)-U(1)-O(4)	49.5(6)	62.90543	61.23153